Exploring the implications of CoCrFeNiCu high entropy alloy coatings on tribomechanical, wetting behavior, and interfacial microstructural characterizations in microwave-clad AISI [Comment: To pgn: Please link author names and affiliations as follows: Shubham Sharma (1)(2)(14), Shashi Prakash Dwivedi (3), Ashutosh Pattanaik (4), Yashwant Singh Bisht (5), Teku Kalyani (6), Vikasdeep Singh Mann (7), Rajeev Kumar (8)(9), Abhinav Kumar (10,11), Drazan Kozak (12), Jasmina Lozanovic (11)(13)

(1) Department of Technical Sciences, Western Caspian University, Baku, Azerbaijan
(2) Centre for Research Impact and Outcome, Chitkara University Institute of Engineering and Technology, Chitkara University, Rajpura 140401, Punjab, India
(3) Department of Mechanical Engineering, Lloyd Institute of Engineering & Technology, Knowledge Park II, Greater Noida, Uttar Pradesh 201306, India
(4) Department of Mechanical Engineering, School of Engineering and Technology, JAIN (Deemed to be University), Bangalore, Karnataka, India
(5) Department of Mechanical Engineering, Uttaranchal Institute of Technology, Uttaranchal University, Dehradun 248007, India
(6) Department of Mechanical Engineering, Raghu Engineering College, Dakamarri 531162, Andhra Pradesh, India
(7) Department of Mechanical Engineering, Chandigarh College of Engineering, Chandigarh Group of Colleges, Jhanjeri, Mohali 140307, Punjab, India
(8) School of Mechanical Engineering, Lovely Professional University, Jalandhar, Punjab, 144001, India

(9) School of Mechanical Engineering, Lovely Professional University, Jalandhar, Punjab, 144001, India
(10) Department of Nuclear and Renewable Energy, Ural Federal University Named After the First President of Russia, Boris Yeltsin, 19 Mira Street, 620002, Ekaterinburg, Russia
(11) Centre for Energy and Environment, Karpagam Academy of Higher Education, Coimbatore, 641021, India
(12) Mechanical Engineering Faculty in Slavonski Brod, University of Slavonski Brod, Trg Ivane Brlić-Mažuranić 2, HR-35000 Slavonski Brod, Croatia
(13) Department of Engineering, University of Applied Sciences Campus Vienna, 1100, Vienna, Austria
(14) Jadara University Research Center, Jadara University, Jordan]Q2Q3Q4 304 stainless steels

The corrections made in this section will be reviewed by journal production editor.

Shubham Sharma, PhD, https://orcid.org/0000-0001-9446-8074, shubham543sharma@gmail.com, Shashi Prakash Dwivedi, spdglb@gmail.com, Ashutosh Pattanaik, Yashwant Singh Bisht, Teku Kalyani, Vikasdeep Singh Mann, Rajeev Kumar, Abhinav Kumar, Drazan Kozak and Jasmina Lozanovic

~~Department of Mechanical Engineering, Lebanese American University, Kraytem 1102-2801, Beirut, Lebanon~~
Department of Technical Sciences, Western Caspian University, Baku, Azerbaijan
Centre for Research Impact and Outcome, Chitkara University Institute of Engineering and Technology, Chitkara University, Rajpura 140401, Punjab, India
Department of Mechanical Engineering, Lloyd Institute of Engineering & Technology, Knowledge Park II, Greater Noida, Uttar Pradesh 201306, India
Department of Mechanical Engineering, School of Engineering and Technology, JAIN (Deemed to be University), Bangalore, Karnataka, India
Department of Mechanical Engineering, Uttaranchal Institute of Technology, Uttaranchal University, Dehradun 248007, India
Department of Mechanical Engineering, Raghu Engineering College, Dakamarri 531162, Andhra Pradesh, India
Department of Mechanical Engineering, Chandigarh College of Engineering, Chandigarh Group of Colleges, Jhanjeri, Mohali 140307, Punjab, India
School of Mechanical Engineering, Lovely Professional University, Jalandhar, Punjab, 144001, India
Department of Nuclear and Renewable Energy, Ural Federal University Named After the First President of Russia, Boris Yeltsin, 19 Mira Street, 620002, Ekaterinburg, Russia
Department of Mechanical Engineering, Karpagam Academy of Higher Education, Coimbatore, 641021, India
Centre for Energy and Environment, Karpagam Academy of Higher Education, Coimbatore, 641021, India

Mechanical Engineering Faculty in Slavonski Brod, University of Slavonski Brod, Trg Ivane Brlić-Mažuranić 2, HR-35000 Slavonski Brod, Croatia

Department of Engineering, University of Applied Sciences Campus Vienna, 1100, Vienna, Austria

Jadara University Research Center, Jadara University, Jordan

Corresponding authors: Shubham Sharma, Department of Mechanical Engineering, Lebanese American University, Kraytem 1102-2801, Beirut, Lebanon; Department of Technical Sciences, Western Caspian University, Baku, Azerbaijan; and Centre for Research Impact and Outcome, Chitkara University Institute of Engineering and Technology, Chitkara University, Rajpura 140401, Punjab, India, E-mail: shubham543sharma@gmail.com, shubhamsharmacsirclri@gmail.com; and **Shashi Prakash Dwivedi**, Department of Mechanical Engineering, Lloyd Institute of Engineering & Technology, Knowledge Park II, Greater Noida, Uttar Pradesh 201306, India, E-mail: spdglb@gmail.com

Corresponding authors: Shubham Sharma, Department of Technical Sciences, Western Caspian University, Baku, Azerbaijan; Centre for Research Impact and Outcome, Chitkara University Institute of Engineering and Technology, Chitkara University, Rajpura 140401, Punjab, India; and Jadara University Research Center, Jadara University, Jordan, E-mail: shubham543sharma@gmail.com; and **Shashi Prakash Dwivedi**, Department of Mechanical Engineering, Lloyd Institute of Engineering & Technology, Knowledge Park II, Greater Noida, Uttar Pradesh 201306, India, E-mail: spdglb@gmail.com

Abstract

The exploration of high-performance coatings is specifically necessary for enhancing the mechanical, thermal, and corrosion-resistant characteristics of structural steels in response to the demand for cutting-edge materials in engineering applications. The current study addresses an existing void in the development of durable coatings that gain benefits from the distinctive characteristics of CoCrFeNiCu high entropy alloys (HEA) for stainless steel substrates, with a particular emphasis on SS 304. The primary objective was to examine the microstructural, mechanical, and corrosion behaviors of SS 304 that had been coated with CoCrFeNiCu HEA employing a microwave cladding process. HEA particles were prepared through mechanical milling, and a controlled cladding process was conducted under an inert environment. A variety of meticulous investigations, including Scanning Electron Microscopy (SEM), X-ray Diffraction (XRD), and wear rate measurements, have been performed to thoroughly assess crucial parameters, including surface hardness, resistance to corrosion, and wear behavior. This study explores the influence of a CoCrFeNiCu high entropy alloy (HEA) coating (20 % each component) on SS-304 steel. Utilizing microwave cladding, the coating demonstrated a substantial impact on wetting behavior, interfacial microstructure, hardness, and corrosion resistance. Surface hardness was substantially enhanced by the cladding process, resulting in a 54.76 % rise from 210 HV to 325 HV. This enhancement substantially raised the mechanical strength of the steel. Under 120 h of corrosion testing in 3.5 wt.% NaCl, a minimal weight loss of 0.342 mg was observed, suggesting that the material exhibited substantial corrosion resistance. In addition, the material's capacity to resist abrasive forces has been demonstrated by the relatively minimal wear rate of 0.0012 mm^3/m that was noticed throughout wear resistance experiments. Effective interfacial adhesion, bonding strength, and uniform distribution were observed by the coating, which resulted in enhanced mechanical characteristics and durability in harsh circumstances. Wetting characteristics indicated enhanced hydrophobicity/hydrophilicity compared to the uncoated surface. SEM images displayed a well-adhered, homogeneous interfacial region, signifying a robust metallurgical bond. The cladding surface exhibited a uniform distribution of CoCrFeNiCu HEA particles. Notably, the steel's surface hardness increased by approximately 54.76 % postdeposition. These findings underscore the potential of CoCrFeNiCu HEA coatings in advancing steel surface properties for improved performance and durability. The potential of CoCrFeNiCu HEA coatings to enhance the performance and longevity of SS 304 steel in chemical, marine environments, etc., applications that necessitate superior resistance to wear, protection against corrosion, and structural or mechanical integrity is underscored by these findings.

Keywords deposition; interfaces; surfaces; microstructure; corrosion

List of abbreviations

SS 304 stainless steel 304

HEA high entropy alloy

CoCrFeNiCu high entropy alloy composed of cobalt (Co), chromium (Cr), iron (Fe), nickel (Ni), and copper (Cu)

SEM scanning electron microscope

XRD X-ray diffraction

HV Vickers hardness

wt.% weight percentage

GHz gigahertz

W watts

s seconds

m/s meters per second

mm^3/m cubic millimeters per meter

°C degree Celsius

NaCl sodium chloride

WC tungsten carbide

AISI American iron and steel institute

Mo_3Si molybdenum silicide

SiC silicon carbide

TiC titanium carbide

Cr_3C_2 chromium carbide

Fe iron

$FeNi_3$ iron nickel intermetallic

Cr_2O_3 chromium oxide

CuO copper oxide

NiCO nickel cobalt oxide

Fe_2O_3 iron oxide

Variables in equations

P probability of a particular system state in the Markov model

λ failure rate of the system components in availability modeling

μ repair rate of the system components in availability modeling

T time variable for different process durations dV/dt rate of change in volume or material removal in wear analysis

t time

L sliding distance

F load

V volume of material removed

S sliding speed

1 Introduction

Stainless Steel 304 (SS 304) is a widely used austenitic stainless steel alloy due to its exceptional corrosion resistance, durability, and versatility. Composed of chromium and nickel, SS 304 exhibits excellent resistance to a variety of corrosive environments, making it ideal for applications in the food industry, medical equipment, architecture, and chemical processing [1]. Its high strength-to-weight ratio and heat resistance further extend its use in automotive components, kitchen appliances, and structural elements [2]. SS 304's nonreactive nature and aesthetic appeal also make it a preferred choice for decorative applications. Its balanced properties make SS 304 a cornerstone material in various industries [3].

CoCrFeNiCu high entropy alloy (HEA) has emerged as a remarkable material with extensive potential for advanced coating applications. Its unique composition, comprising multiple elements in roughly equal proportions, contributes to its exceptional mechanical, thermal, and chemical properties [4]. HEA coatings offer a versatile solution for enhancing the surface performance of various substrates. With remarkable wear resistance, hardness, and corrosion resistance, HEA coatings find utility in industries such as aerospace, automotive, energy, and manufacturing. The excellent thermal stability of HEA coatings makes them suitable for high-temperature applications, including turbine blades and exhaust systems. Their resistance to oxidation and harsh environments extends the lifespan of coated components. HEA coatings also display promising biocompatibility, making them candidates for medical implants and devices [5].

While there has been significant research on the development of high entropy alloy (HEA) coatings and their various applications, there exists a noticeable gap in the literature regarding the specific influence of CoCrFeNiCu HEA coatings on the wetting behavior and interfacial microstructure of SS 304 steel surfaces, particularly when developed using microwave cladding [6]. Existing studies often focus on the mechanical and corrosion properties of HEA coatings, but the intricate relationship between HEA coatings, wetting behavior, and interfacial microstructure on SS 304 steel surfaces remains relatively unexplored [7], [8]. Additionally, the novel application of microwave cladding to deposit HEA coatings introduces a unique aspect that requires further investigation in terms of its impact on coating properties and interactions with the substrate [9], [10].

Microwave energy has emerged as a powerful tool in cladding processes, particularly for enhancing the wear resistance and surface properties of steel. In a comprehensive review by Singh et al. [11], the efficacy of microwave cladding in countering slurry erosion wear was underscored. The importance of protective coatings to mitigate erosion damage was emphasized, leading to a growing interest in exploring microwave cladding techniques. One notable study by Durga Prasad et al. [12] utilized CoMoCrSi + Flyash for cladding on AISI 410 steel through microwave irradiation. This process, conducted at 900 W and 2.45 GHz for 1,800 s, resulted in the formation of hard phases like Mo_3Si, SiC, TiC, Co_3Ti, and Cr_3C_2, as confirmed by XRD analysis. The presence of an oxide layer substantially enhanced wear resistance. In a different approach, Singh et al. [13] employed a modified B-type thermocouple to develop Ni-based clads, allowing real-time temperature distribution measurement. Microwave clads on AISI 420 by Vishwanatha et al. [14] demonstrated superior erosion resistance compared to the substrate after a 7-min exposure. Meanwhile, Kumar et al. [15] improved the properties of austenitic stainless steel by cladding with nickel, significantly enhancing oxidation and wear resistance. Despite noting a thin oxide layer on the clad surface, there was a notable increase in microhardness. The impact of heat treatment on Ni-based microwave cladding was explored by Singh et al. [16], revealing the partial dissolution of eutectic carbides at 1,000 °C. Mishra et al. [17] deposited Ni and Ni-WC cladding on low carbon steel, demonstrating that a 12 wt.% accumulation of WC improved abrasive wear and hardness. Further diversifying the cladding materials, Babu et al. [18] synthesized Ni–SiC composite claddings, exhibiting exceptional erosion resistance with both brittle and ductile erosion mechanisms observed. Nair et al. [19] developed AlxCoCrFeNi high entropy alloy claddings using microwave heating, showcasing significantly reduced erosion rates compared to SS316L steel. Nanostructured clads were the focus of research by Zafar et al. [20], who observed a uniform distribution of nanocarbides, resulting in high flexural strength and microhardness. Hebbale et al. [21] contributed to the field by developing Ni-based cladding on austenitic SS 304 through microwave irradiation, revealing a microhardness of 364 ± 70 HV, attributed to well-distributed intermetallic and metal carbides, along with reduced porosity. These studies collectively highlight the diverse and promising applications of microwave energy in enhancing the properties of clad materials for improved wear resistance and surface performance in various industrial contexts.

This study aims to bridge the existing literature gap by investigating the specific effects of CoCrFeNiCu HEA coatings on the wetting behavior and interfacial microstructure of SS 304 steel surfaces, with a focus on coatings developed through microwave cladding. The novelty of this research lies in the combination of two relatively underexplored areas: the impact of HEA coatings on wetting behavior and interfacial microstructure, and the innovative application of microwave cladding for HEA coating deposition. By examining these aspects in conjunction, this study seeks to uncover novel insights into how CoCrFeNiCu HEA coatings influence the surface characteristics of SS 304 steel and the underlying mechanisms governing their interfacial interactions. This research has the potential to contribute to the broader understanding of HEA coatings and their tailored applications in surface engineering.

2 Experimentation: materials and methods

Figure 1(a) shows the powder SEM image of ball-milled CoCrFeNiCu HEA particles. The image exhibited a complex structure with varying particle sizes, indicating the effects of ball milling on particle morphology. The mechanical milling process had induced a combination of smaller and more refined particles along with some agglomerates. The cladding process of CoCrFeNiCu HEA on SS 304 was carried out by microwave energy (Figure 1(b)). The SS 304 steel substrate was cleaned thoroughly to remove any dirt, grease, or oxide layers. The substrate's surface was polished to ensure proper adhesion of the HEA coating. The CoCrFeNiCu HEA powder in equal weight percent was ball-milled. The polished SS 304 substrate was securely fixed and cleaned in the cladding setup, ensuring proper alignment and positioning. The cladding chamber with argon gas was purged to create an inert atmosphere that prevented oxidation during the cladding process. The CoCrFeNiCu HEA powder was loaded into a controlled feeding mechanism within the cladding setup. The microwave heating process was initiated to melt the SS 304 for coating HEA powder. After the coating was deposited, the system was allowed to cool gradually under the argon atmosphere to prevent rapid cooling-induced stress and cracking. Figure 2(a) and (b) shows the photograph and SEM image of 304 without cladding. Figure 3(a)–(c) shows the photograph of CoCrFeNiCuHEA particles, SEM image of CoCrFeNiCuHEA particles, and XRD of CoCrFeNiCuHEA particles. Figure 4 shows the samples with corrosion testing, and hardness testing indentation must be shown in schematic images.

Figure alignment: The figure layout displayed in this section is not how it will appear in the final version. As per journal style, figures will only be left aligned. The presentation below is for the sole purpose of providing corrections to the figures. To view the actual presentation of the figures, please click on the PDF located at the top of the page.

Figure 1:

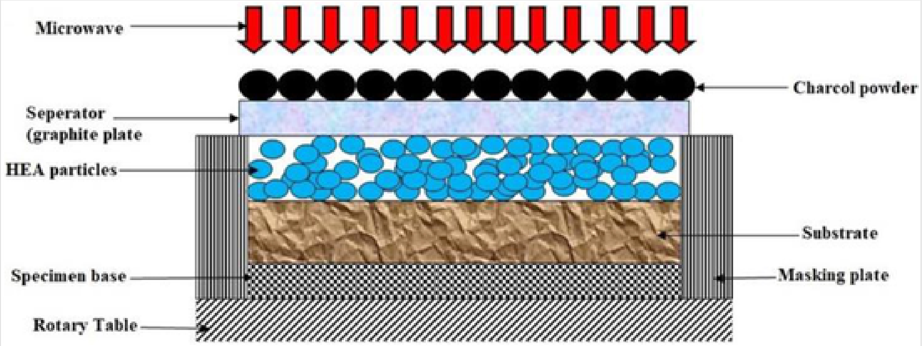

Microwave process.

Figure alignment: The figure layout displayed in this section is not how it will appear in the final version. As per journal style, figures will only be left aligned. The presentation below is for the sole purpose of providing corrections to the figures. To view the actual presentation of the figures, please click on the PDF located at the top of the page.

Figure 2:

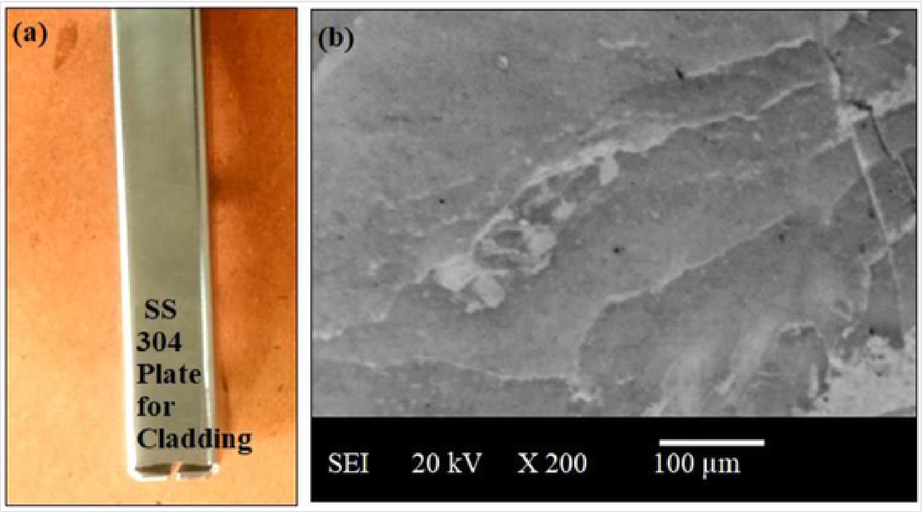

Q5 ~~Fig.2.~~ Photograph and micrograph, (a) Photograph of SS 304 and (b) SEM image of 304 without cladding.

Figure alignment: The figure layout displayed in this section is not how it will appear in the final version. As per journal style, figures will only be left aligned. The presentation below is for the sole purpose of providing corrections to the figures. To view the actual presentation of the figures, please click on the PDF located at the top of the page.

Figure 3:

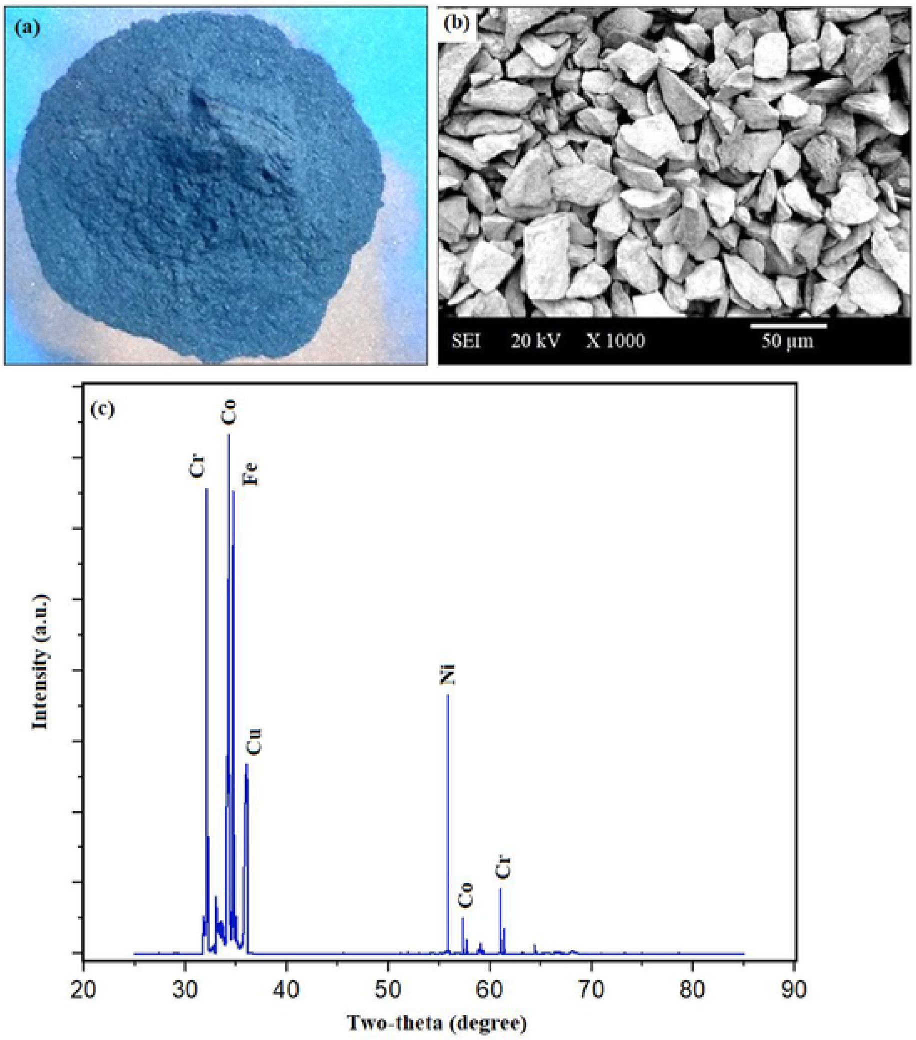

~~Fig.3.~~(a) Photograph and microstructural analysis, Photograph of CoCrFeNiCuHEA particles, (b) SEM image of CoCrFeNiCuHEA particles, and (c) XRD of CoCrFeNiCuHEA particles.

Figure alignment: The figure layout displayed in this section is not how it will appear in the final version. As per journal style, figures will only be left aligned. The presentation below is for the sole purpose of providing corrections to the figures. To view the actual presentation of the figures, please click on the PDF located at the top of the page.

Figure 4:

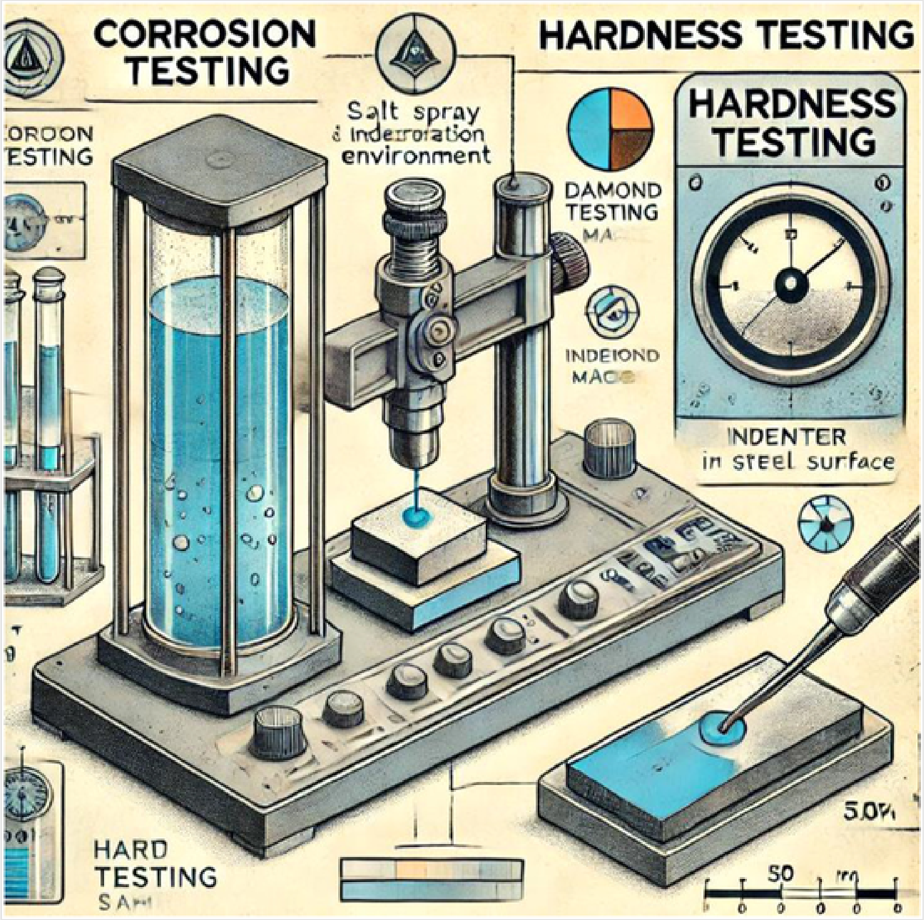

The samples with corrosion testing, hardness testing indentation must be shown in schematic images.

3 Results and discussions

3.1 Microstructure analysis

A representative sample of the CoCrFeNiCuHEA particles on SS 304 was chosen to ensure it accurately reflects the overall microstructure of the material. The selected sample was mounted in a thermosetting resin to facilitate handling and protect the edges during subsequent preparation steps. The mounted sample was sectioned using a precision saw to obtain a flat and smooth surface, minimizing damage and deformation. The sectioned sample underwent grinding using progressively finer silicon carbide papers, starting with coarse grit (e.g., 240 grit) and moving to finer grits (e.g., 1,200 Q6 grit). This step was crucial for removing surface irregularities and scratches [78], [79]. After grinding, the sample was polished using alumina or diamond suspensions on polishing cloths. This process continued until a mirror-like finish was achieved, essential for clear microstructural observation [80]. The polished sample was then etched using a suitable chemical reagent, such as Keller's reagent, to reveal the microstructure. Etching selectively attacks certain phases, making grain boundaries and different phases visible under a microscope [81]–[83]. Postetching, the sample was thoroughly cleaned with distilled water and alcohol to remove any residual etchant and debris, preventing contamination during analysis [84]. The prepared sample was examined under an optical microscope and possibly an SEM analysis to observe and document the microstructure. Features such as grain size, phase distribution, and the presence of any secondary phases or defects were analyzed [85], [86]. Figure 5 shows the wetting and interfacial behavior between the substrate (SS 304) and cladding surface coating with CoCrFeNiCu high entropy alloy. The wetting and interfacial behavior between the substrate (SS 304) and the cladding surface coating with CoCrFeNiCu high entropy alloy (HEA) played a pivotal role in determining the coating's overall performance and the durability of the cladding surface structure. Wetting refers to the ability of a liquid or molten material to spread across a solid surface. In the context of coating deposition in this study, wetting behavior directly affected the uniformity of the coating layer. The wetting behavior between molten SS 304 and the CoCrFeNiCu HEA was influenced by surface energy and interfacial tension. It was observed that when the HEA coating exhibited good wetting, it was spread uniformly over the SS 304 substrate, resulting in a continuous and defect-free coating. Proper wetting was crucial for achieving strong adhesion and minimizing the risk of delamination or cracks forming at the interface. The interfacial behavior between the SS 304 substrate and the CoCrFeNiCu HEA coating is characterized by the quality of bonding, diffusion of atoms, and potential formation of intermetallic compounds [22], [23]. A strong and well-bonded interface is essential to ensure mechanical integrity and to prevent separation under external forces or thermal cycling. The interfacial microstructure, including any intermetallic phases formed, can significantly influence mechanical properties and corrosion resistance. In this study, interfacial diffusion between the substrate and coating materials led to the development of a diffusion zone at the interface. This zone exhibited altered mechanical and chemical properties compared to the substrate. It has been observed that interfacial behavior between the substrate (SS 304) and cladding surface ensured improved adhesion, minimized defects, and optimized mechanical properties. Figure 6(a) and (b) shows the SEM image of the coating surface of SS 304 deposited with CoCrFeNiCu high entropy alloy. Achieving uniform distribution and porosity-free cladding of CoCrFeNiCu high entropy alloy onto SS 304 is paramount for optimal performance. In this study, uniform distribution of CoCrFeNiCu HEA particles with porosity-free surfaces was observed. A uniform distribution ensured consistent material properties across the coated surface, enhancing mechanical strength and corrosion resistance (Figure 3(c) and (d)). Eliminating porosity prevented the ingress of corrosive agents and reduced the risk of structural weaknesses. Figure 7 shows the EDS mapping results at the interface region of cladding.

Figure alignment: The figure layout displayed in this section is not how it will appear in the final version. As per journal style, figures will only be left aligned. The presentation below is for the sole purpose of providing corrections to the figures. To view the actual presentation of the figures, please click on the PDF located at the top of the page.

Figure 5:

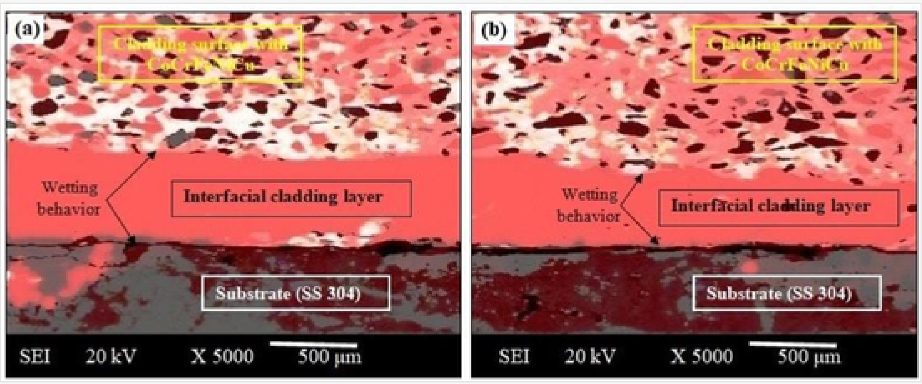

~~Fig.5.~~Microstructural morphology analysis, (a and b) Wetting and interfacial behavior between the substrate (SS 304) and cladding surface coating with CoCrFeNiCu high entropy alloy.

Figure alignment: The figure layout displayed in this section is not how it will appear in the final version. As per journal style, figures will only be left aligned. The presentation below is for the sole purpose of providing corrections to the figures. To view the actual presentation of the figures, please click on the PDF located at the top of the page.

Figure 6:

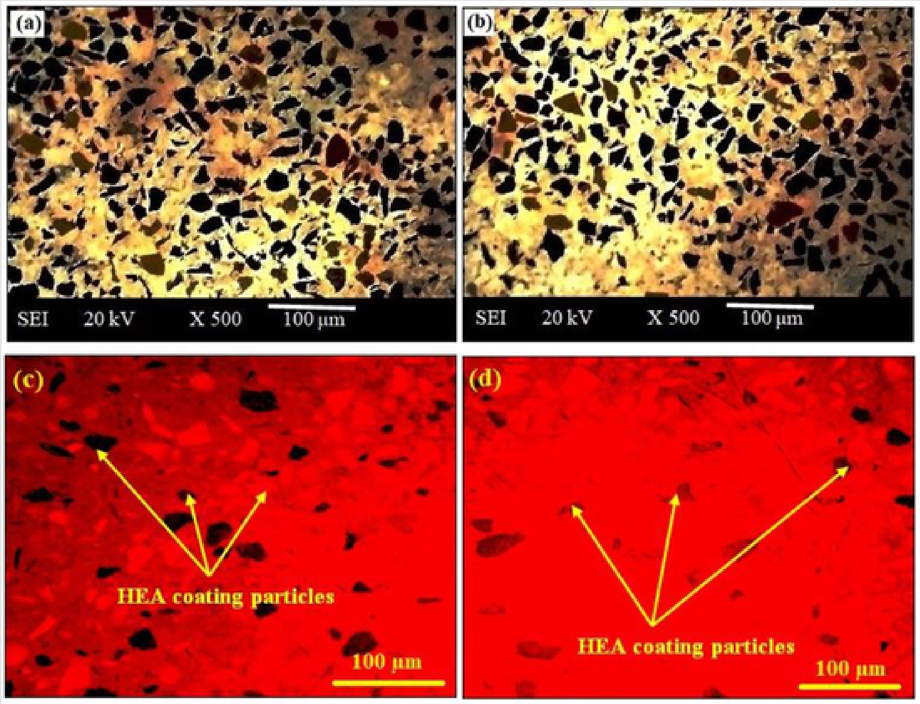

~~Fig.6.~~ Morphology analysis, (a and b) SEM image of coating surface of SS 304 deposited with CoCrFeNiCu high entropy alloy. (c and d) Optical microscopic image of coating surface of SS 304 deposited with CoCrFeNiCu high entropy alloy.

i **Figure alignment:** The figure layout displayed in this section is not how it will appear in the final version. As per journal style, figures will only be left aligned. The presentation below is for the sole purpose of providing corrections to the figures. To view the actual presentation of the figures, please click on the PDF located at the top of the page.

Figure 7:

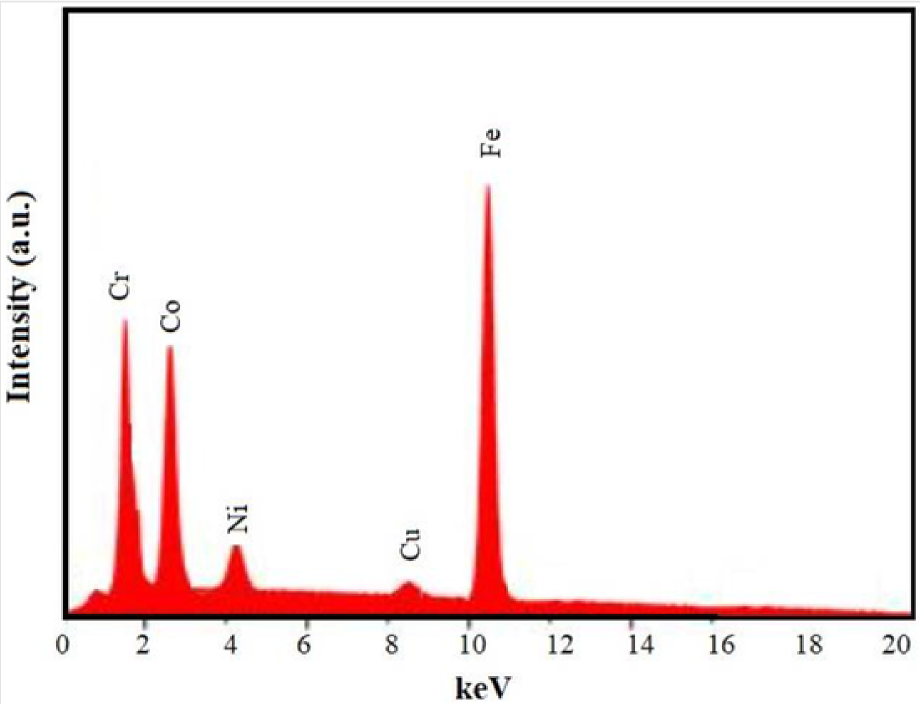

The EDS mapping results at the interface region of cladding.

The number of grains for the substrate (SS 304) coating with CoCrFeNiCu high entropy alloy per square inch at 500 magnification was identified. The number of grains (n) was observed by following Equation (1):

$$n = 2^{(G-1)} \tag{1}$$

where, n = the number of grains, G = grain size number ASTM.

$$G = \left[-6.644 \log_{10}\left(l_\alpha\right)\right] - 3.28 \tag{2}$$

where, $l_\alpha = \frac{V_{v\alpha}(L_T)}{N_\alpha}$

Here, $V_{v\alpha}$ = fraction of α phase (volume), L_T = length/magnification (test line), N_α = grains intercepted (number). Now,

$$l_\alpha = \frac{0.48 \times (487/500)}{94},$$

$$l_\alpha = 0.00497$$

Now again G from Equation (2),

$$G = \left[-6.644 \log_{10}(0.00497)\right] - 3.28$$

$$G = 12.025$$

Now from Equation (1)

$$n = 2^{(12.025-1)}$$

$$n = 2^{(11.025)}$$

$$n = 2,083.79$$

The substrate (SS 304) coating with CoCrFeNiCu high entropy alloy exhibited approximately 2,083.79 grains per square inch at 500× magnification. This high grain count indicates the formation of a finer grain structure, which is beneficial for enhancing the coating's mechanical properties such as hardness and wear resistance. Finer grains often contribute to improved strength and durability, making the coating more suitable for demanding applications. The observed grain size, with approximately 2,083.79 grains per square inch at 500× magnification, signifies a finer grain structure, which plays a crucial role in enhancing the mechanical properties of the composite material. Smaller grain sizes increase the material's hardness and strength due to the grain boundary strengthening mechanism, also known as the Hall–Petch effect. This result suggests that the high entropy alloy coating successfully refined the grain structure on the SS 304 substrate, potentially improving its performance in various industrial uses.

3.2 Surface hardness

ASTM E92 – Standard Test Method was used for Vickers hardness. Load during the Vickers hardness was 100 kgf and dwell time was 15 s. The inherent hardness of SS 304 steel was measured at 210 HV. However, through the process of cladding with CoCrFeNiCu high entropy alloy (HEA), the surface hardness of SS 304 significantly increased to 325 HV. Figure 7 shows the hardness distribution of substrate, cladding layer, and cladding surface. This remarkable enhancement represents a notable 54.76% improvement in the surface hardness of SS 304 after the incorporation of CoCrFeNiCu HEA. The substantial increase in hardness was a clear indication of the effectiveness of HEA particles in reinforcing the mechanical properties of the steel. The unique composition and characteristics of the CoCrFeNiCu HEA, known for its high entropy and uniform distribution of multiple elements, played a pivotal role in enhancing the hardness of the clad material [22], [23]. This improvement in surface hardness was of considerable significance, as it suggested that cladding with CoCrFeNiCu HEA resulted in a steel alloy with superior mechanical strength, potentially making it well-suited for applications where increased hardness and durability are essential as Q7 depicted in figure 8Figure 8. (Figure 8).

Figure alignment: The figure layout displayed in this section is not how it will appear in the final version. As per journal style, figures will only be left aligned. The presentation below is for the sole purpose of providing corrections to the figures. To view the actual presentation of the figures, please click on the PDF located at the top of the page.

Figure 8:

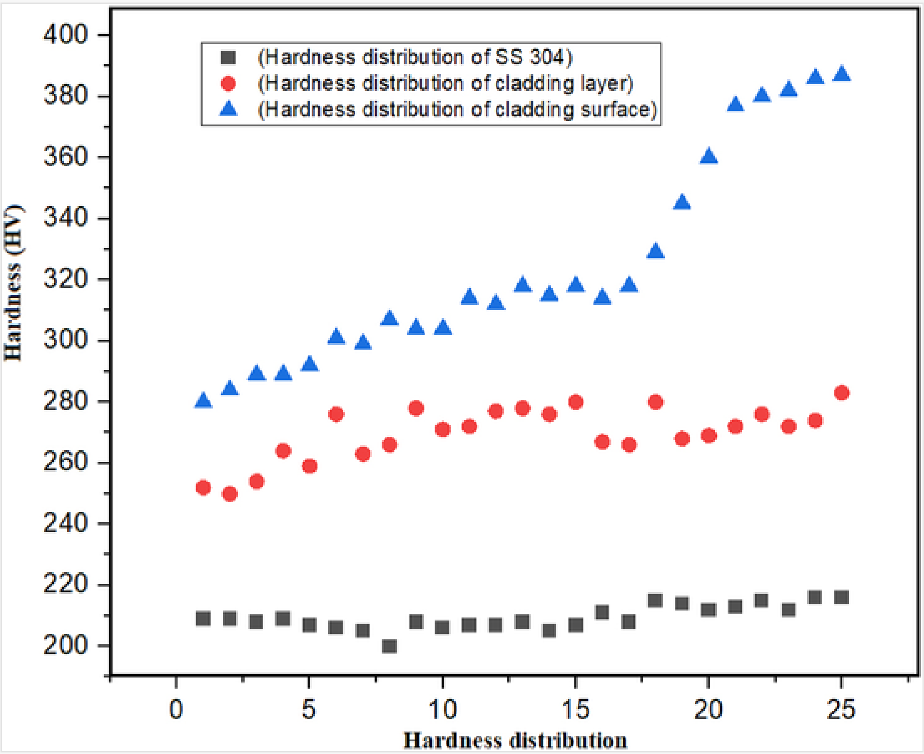

Hardness distribution of substrate, cladding layer, and cladding surface.

3.3 Corrosion behavior

Figure 9 shows corroded surface SEM image of SS 304 without cladding of CoCrFeNiCu high entropy alloy. In Figure 10(a), the corrosion surface behavior of SS 304, deposited with a CoCrFeNiCu high entropy alloy (HEA), is elucidated. A corrosion test conducted in 3.5 wt.% NaCl for 120 h revealed a corrosion weight loss of 0.342 mg for SS 304 steel with the CoCrFeNiCu HEA coating. The SEM image vividly displayed the corrosion behavior of SS 304 steel after being coated with the high entropy alloy. Notably, the CoCrFeNiCu HEA particles contributed to enhanced protection by forming a dense and protective layer on the steel surface, thereby reducing its susceptibility to corrosion. The SEM analysis served as compelling evidence for improved corrosion resistance, showcasing the potential for an extended material lifespan. The observed protective layer acted as a barrier, mitigating the corrosive effects of the environment [22], [23]. This finding is crucial for applications where corrosion resistance is paramount, such as in marine or chemical environments, suggesting that the incorporation of CoCrFeNiCu HEA through deposition on SS 304 steel can significantly enhance its durability and longevity in challenging conditions.

Figure alignment: The figure layout displayed in this section is not how it will appear in the final version. As per journal style, figures will only be left aligned. The presentation below is for the sole purpose of providing corrections to the figures. To view the actual presentation of the figures, please click on the PDF located at the top of the page.

Figure 9:

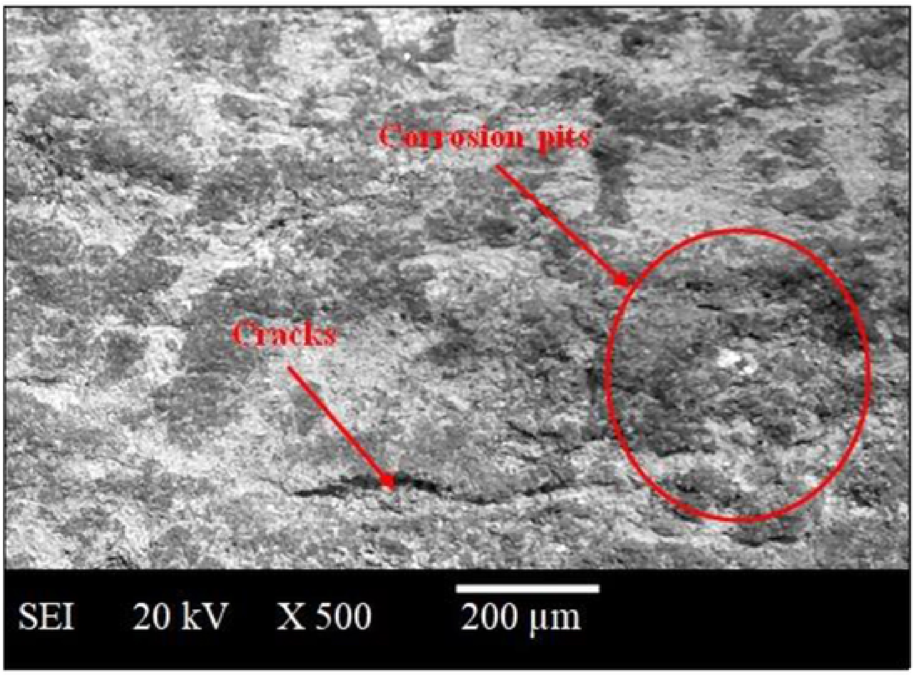

Corroded surface SEM image of SS 304 without cladding of CoCrFeNiCu high entropy alloy.

Figure alignment: The figure layout displayed in this section is not how it will appear in the final version. As per journal style, figures will only be left aligned. The presentation below is for the sole purpose of providing corrections to the figures. To view the actual presentation of the figures, please click on the PDF located at the top of the page.

Figure 10:

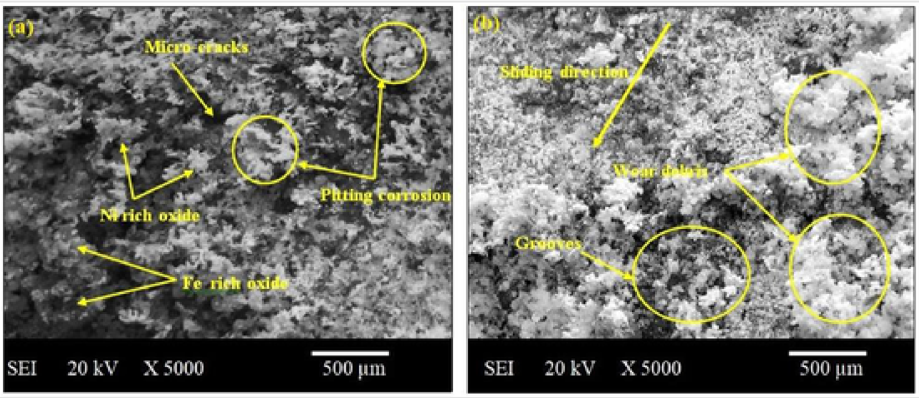

~~Fig.10.~~ Morphology analysis, (a) Corroded surface SEM image of SS 304 deposited with CoCrFeNiCu high entropy alloy and (b) worn surface behavior of SS 304 deposited with CoCrFeNiCu high entropy alloy.

3.4 Wear behavior

ASTM G99 – Standard Test Method was used for Wear Testing with a Pin-on-Disk Apparatus. The wear test of the coated surface was meticulously conducted using a pin-on-disc machine, employing specific parameters such as a sliding speed of 2 m/s, a sliding distance of 1,000 m, and a load of 15 N. The results yielded an exceptionally low wear rate for the coating material, measuring a mere 0.0012 mm^3/m. This remarkably low wear rate was a testament to the coating's exceptional resistance to wear and friction, establishing it as a highly durable and promising material for applications where minimizing material loss and prolonging the lifespan of components is of utmost importance. Upon examination of the worn surface of the coating, evident signed of wear manifested in the form of wear debris and grooves, as illustrated in Figure 10(b). These visible features pointed toward the abrasive nature of the wear process, where material has been actively removed and displaced, resulting in the formation of grooves. The presence of wear debris and grooves was indicative of the coating undergoing substantial mechanical stress and friction during the wear test [22], [23]. Despite the wear, the coating's low wear rate underscored its robustness and capability to withstand the challenges of abrasive wear, highlighting its potential for applications demanding high wear resistance and durability. This comprehensive wear analysis solidified the coating's merit as a reliable choice for components subjected to frictional forces, demonstrating its capacity to endure and maintain performance integrity over prolonged operational periods.

3.5 XRD analysis

The X-ray diffraction (XRD) analysis of the SS 304 coating with CoCrFeNiCu high entropy alloy reveals a complex composition characterized by the presence of distinct crystalline phases (Figure 11). The prominent peaks in the XRD pattern indicated the existence of Fe (iron), $FeNi_3$, Cr_2O_3 (chromium oxide), CuO (copper oxide), NiCO, and Fe_2O_3 (iron oxide). The detection of Fe suggested the incorporation of iron into the alloy structure, contributing to its mechanical and magnetic properties. The presence of $FeNi_3$ indicated the formation of a nickel-rich intermetallic phase, potentially enhancing the alloy's strength and corrosion resistance. Cr_2O_3 signified the presence of chromium oxide, contributing to the alloy's oxidation resistance. The identification of CuO and NiCO suggested the oxidation of copper and nickel, respectively, which were implications for the alloy's stability under different environmental conditions. The presence of Fe_2O_3, an iron oxide, indicated the potential occurrence of surface oxidation, influencing the alloy's overall performance.

Figure 11:

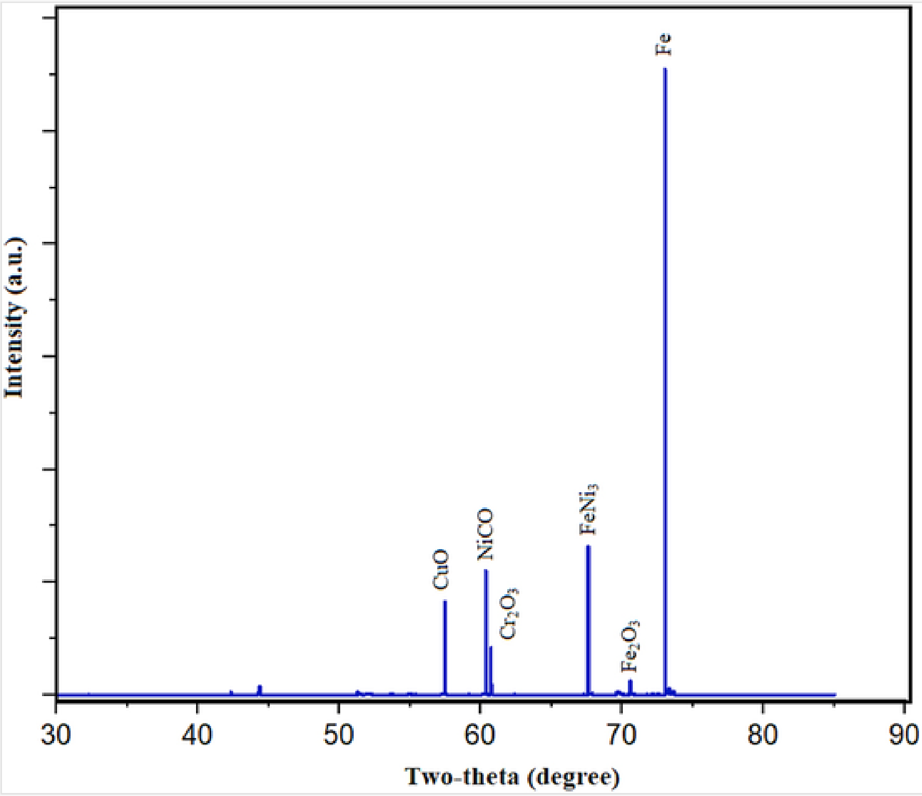

XRD of coating samples.

4 Conclusions

This study delves into the profound influence of CoCrFeNiCu high entropy alloy (HEA) coating on various properties of SS 304 steel, employing a microwave cladding technique. The HEA coating not only exhibited remarkable alterations in wetting behavior, emphasizing its potential for tailored surface properties but also demonstrated excellent interfacial bonding. The substantial 54.76 % enhancement in surface hardness after cladding CoCrFeNiCu HEA underscored its capacity to reinforce the steel's mechanical properties. Additionally, the corrosion test in 3.5 wt.% NaCl for 120 h revealed minimal weight loss (0.342 mg) for SS 304 steel with CoCrFeNiCu HEA coating, attesting to its corrosion resistance. In wear testing, the coating exhibited a remarkably low wear rate (0.0012 mm^3/m) under specific conditions, indicating its outstanding wear resistance. This research elucidates the intricate relationship between HEA coatings, wetting behavior, interfacial interactions, and their practical implications for enhancing the performance and durability of steel materials in various engineering applications.

References

The corrections made in this section will be reviewed by journal production editor.

Q9 [1] A. K. Sharma, S. Aravindhan, and R. Krishnamurthy, "Microwaveglazing of alumina–titania ceramic composite coatings," *Mater. Lett.*, vol. 50, no. 5–6, pp. 295–301, 2011. https://doi.org/10.1016/s0167-577x(01)00243-9.

[2] S. Zhou, X. Zeng, H. Qianwu, and S. Huang, "Analysis of crack behavior for Ni-based WC composite coatings by lasercladding and crack-free realization," *Appl. Surf. Sci.*, vol. 255, no. 5, pp. 1646–1653, 2008. https://doi.org/10.1016/j.apsusc.2008.04.003.

[3] R. C. Leonelli, P. Veronesi, L. Denti, A. Gatto, and L. Iuliano, "Microwave assisted sintering of green metal parts," *J. Mater. Process. Technol.*, vol. 205, no. 1–3, pp. 489–496, 2008. https://doi.org/10.1016/j.jmatprotec.2007.11.263.

[4] J. Mateos, J. M. Cuetos, E. Fernandez, and R. Vijande, "Tribological behavior of plasma-sprayed WC coatings with and without laser remelting," *Wear*, vol. 239, no. 2, pp. 274–281, 2000. https://doi.org/10.1016/s0043-1648(00)00325-2.

[5] D. Roy Agrawal, J. Cheng, and S. Gedevanishvili, "Full sintering of powdered-metal bodies in a microwave field," *Nature*, vol. 339, pp. 668–670, 1999. https://doi.org/10.1038/21390.

[6] A. Mondal, A. Upadhyaya, and D. Agrawal, "Microwave sintering of refractory metals/alloys," *J. Microw. Power Electromagn. Energy*, vol. 44, no. 1, pp. 28–44, 2009. https://doi.org/10.1080/08327823.2010.11689768.

[7] D. Gupta, A. K. Sharma, P. M. Bhovi, and S. Dutta, "Development and characterization of microwave composite cladding," *J. Manuf. Process.*, vol. 14, no. 3, pp. 243–249, 2012. https://doi.org/10.1016/j.jmapro.2012.05.007.

[8] M. Tlotleng, E. Akinlabi, M. Shukla, and S. Pityana, "Microstructure, hardness and bioactivity of hydroxyapatite coatings deposited by direct laser melting process," *Mater. Sci. Eng. C*, vol. 43, pp. 189–198, 2014. https://doi.org/10.1016/j.msec.2014.06.032.

[9] S. P. Dwivedi, S. Sharma, and S. Sharma, "Identification of microwave radiation effect on copper welded joint with brass as filler material using response surface methodology," *Mater. Perform. Charact.*, vol. 9, no. 1, pp. 267–276, 2020. https://doi.org/10.1520/mpc20190253.

[10] S. P. Dwivedi, S. Sharma, T. Singh, and N. Kumar, "Mechanical and metallurgical characterization of copper-based welded joint using brass as filler metal developed by microwave technique," *Ann. Chimie Sci. Matériaux*, vol. 44, pp. 281–286, 2020. https://doi.org/10.18280/acsm.440407.

[11] B. Singh and S. Zafar, "Microwave cladding for slurry erosion resistance applications: a review," *Mater. Today: Proc.*, vol. 46, no. 7, pp. 2686–2690, 2021. https://doi.org/10.1016/j.matpr.2021.02.371.

[12] C. D. Prasad, M. S. Lingappa, S. Joladarashi, M. R. Ramesh, and B. Sachin, "Characterization and sliding wear behavior of CoMoCrSi + flyash composite cladding processed by microwave irradiation," *Mater. Today: Proc.*, vol. 46, no. 7, pp. 2387–2391, 2021. https://doi.org/10.1016/j.matpr.2021.01.156.

[13] B. Singh and S. Zafar, "Understanding time-temperature characteristics in microwave cladding," *Manuf. Lett.*, vol. 25, pp. 75–80, 2020. https://doi.org/10.1016/j.mfglet.2020.08.002.

[14] J. S. Vishwanatha, A. M. Hebbale, N. Kumar, M. S. Srinath, and R. I. Badiger, "ANOVA studies and control factors effect analysis of cobalt based microwave clad," *Mater. Today: Proc.*, vol. 46, no. 7, pp. 2409–2413, 2021. https://doi.org/10.1016/j.matpr.2021.01.214.

[15] K. P. Kumar, A. Mohanty, M. Shashank Lingappa, M. S. Srinath, and S. K. Panigrahi, "Enhancement of surface properties of austenitic stainless steel by nickel based alloy cladding developed using microwave energy technique," *Mater. Chem. Phys.*, vol. 256, p. 123657, 2020. https://doi.org/10.1016/j.matchemphys.2020.123657.

[16] B. Singh and S. Zafar, "Influence of post clad heat treatment on microstructure and slurry erosion characteristics of Ni-based microwave clad," *Vacuum*, vol. 184, p. 109946, 2021. https://doi.org/10.1016/j.vacuum.2020.109946.

[17] T. K. Mishra, A. Kumar, and S. K. Sinha, "Investigation of sliding wear behaviour of Ni-WC microwave cladding," *Mater. Today: Proc.*, vol. 26, no. 2, pp. 1418–1422, 2020. https://doi.org/10.1016/j.matpr.2020.02.294.

[18] A. Babu, H. S. Arora, H. Singh, and H. S. Grewal, “Microwave synthesized composite claddings with enhanced cavitation erosion resistance,” *Wear*, vol. 422–423, pp. 242–251, 2019. https://doi.org/10.1016/j.wear.2019.01.072.

[19] R. B. Nair, H. S. Arora, A. V. Boyana, P. Saiteja, and H. S. Grewal, “Tribological behavior of microwave synthesized high entropy alloy claddings,” *Wear*, vol. 436–437, p. 203028, 2019. https://doi.org/10.1016/j.wear.2019.203028.

[20] S. Zafar and A. K. Sharma, “Structure-property correlations in nanostructured WC–12Co microwave clad,” *Appl. Surf. Sci.*, vol. 370, pp. 92–101, 2016. https://doi.org/10.1016/j.apsusc.2016.02.114.

[21] A. M. Hebbale and M. S. Srinath, “Microstructural investigation of Ni based cladding developed on austenitic SS-304 through microwave irradiation,” *J. Mater. Res. Technol.*, vol. 5, no. 4, pp. 293–301, 2016. https://doi.org/10.1016/j.jmrt.2016.01.002.

[22] S. P. Dwivedi, et al., “Homogeneity, metallurgical, mechanical, wear, and corrosion behavior of Ni and B4C coatings deposited on 304 stainless steels developed by microwave cladding technique,” *J. Mater. Res. Technol.*, vol. 27, pp. 5854–5867, 2023. https://doi.org/10.1016/j.jmrt.2023.10.202.

Q1 [23] S. P. Dwivedi and S. Sharma, “Synthesis of high entropy alloy AlCoCrFeNiCuSn reinforced $AlSi_7Mg_{0.3}$ based composite developed by solid state technique,” *Mater. Lett.*, vol. 355, p. 135556, 2024. https://doi.org/10.1016/j.matlet.2023.135556.

Footnotes

Text Footnotes

Q8 **Research ethics:** Not applicable.

[Comment: To pgn: Please add "**Informed consent:** Not applicable." above author contribution.]**Author contributions:** Conceptualization, SPD, SS, AMK, RK, YSB; methodology, SPD, SS, AMK, RK, YSB; formal analysis, SPD, SS, AMK, RK, YSB; investigation, SPD, SS, AMK, RK, YSB; writing – original draft, SPD, SS, AMK, RK, YSB; writing – review and editing, SS, TK, AK, MA; supervision, SS, TK, AK, MA; project administration, SS, TK, AK, MA; funding acquisition, SS, TK, AK, MA. All authors have read and agreed to the published version of the manuscript.

[Comment: To pgn: Please add "**Use of Large Language Models, AI and Machine Learning Tools:** None declared." above conflict of interest.]**Conflict of interest:** The authors declare no competing interests.

Research funding: The authors extend their appreciation to the Deanship of Scientific Research at King Khalid University (KKU) for funding this research through the Research Group Program Under the Grant Number: (R.G.P.2/517/44).

Data availability: My manuscript has no associate data.

Queries and Answers

Q1

Query: Please note that the short title will be used as running head on top of the pages. Hence check the retained short title or provide the short title fewer than 75 characters including space.

Answer: I CONFIRM THE SAME.

Q2

Query: As per De Gruyter policy, no author list changes are permitted after acceptance of an article. The De Gruyter production team is instructed to enforce this policy during the production/proofing process.

Answer: I CONFIRM THE SAME. THE AUTHORS HAVE FOLLOWED ALL SORTS OF RESEARCH ETHICAL AND INTEGRITY NORMS AS PER THE STANDARD COPE GUIDELINES.

Q3

Query: Please confirm that the forename(s) and surname(s) have been identified correctly and please carefully verify the spelling of all authors' names.

Answer: I CONFIRM THE SAME.

Q4

Query: Please note that as per the journal style, only one email address should be included for the corresponding author (Shubham Sharma). Kindly check and advise on the one to be retained.

Answer: Kindly consider, shubham543sharma@gmail.com only.

Q5

Query: Please be noted that we expect a figure caption with a main title followed by the description of the part labels. Hence, could you please provide main title captions for "Figures 2, 3, 5, 6, 10" to proceed.

Answer: Fig.2. (a) Photograph of SS 304 and (b) SEM image of 304 without cladding.

Fig.3. (a) Photograph of CoCrFeNiCuHEA particles, (b) SEM image of CoCrFeNiCuHEA particles, and (c) XRD of CoCrFeNiCuHEA particles.

Fig.5.(a-b). Wetting and interfacial behavior between the substrate (SS 304) and cladding surface coating with CoCrFeNiCu high entropy alloy.

Fig.6. (a-b) SEM image of coating surface of SS 304 deposited with CoCrFeNiCu high entropy alloy. (c-d) Optical microscopic image of coating surface of SS 304 deposited with CoCrFeNiCu high entropy alloy.

Fig.10. (a). Corroded surface SEM image of SS 304 deposited with CoCrFeNiCu high entropy alloy, and (b) worn surface behavior of SS 304 deposited with CoCrFeNiCu high entropy alloy.

Q6

Query: References [78]–[86] are cited in the text but not provided in the reference list. Please provide them in the reference list or alternatively delete the citations from the text.

Answer: We have deleted these references since it's a typo error.

Q7

Query: Please note that 'Figure 8' was not cited in the text. Please check that the citation suggested by the copyeditor is in the appropriate place, and correct if necessary.

Answer: Modified

Q8

Query: Please note that we have received the Template for Ethical and Legal Declarations for author statements for this item without headings "Informed consent, Use of Large Language Models, AI and Machine Learning Tools". Please check and provide the missing headings following style. You can download the template here: https://degruyter.knack.com/joda-20#template-for-ethical-and-legal-declarations/.

Answer: Informed consent: Not applicable

Use of Large Language Models, AI and Machine Learning Tools: None declared

Q9

Query: Please provide the issue number for the bibliography in the references [1]–[20], [22], [23].

Answer: I confirm the same.